Multi-Fidelity Uncertainty Quantification for Gas-Solid Flows

Yuan Yao, Xun Huan, and Jesse Capecelatro
University of Michigan, Ann Arbor

2021 NETL Workshop on Multiphase Flow Science
Tuesday, Aug 03, 2021

Gas-solid flows are key to many chemical processes

Fluidized bed reactors are at the heart of nearly all chemical transformation processes

- Conventional technologies: Catalytic-like processes (*e.g.*, **FCC**) remain the primary conversion technique within petrochemical industry
- Emerging technologies: biomass pyrolysis, zero-carbon coal combustion

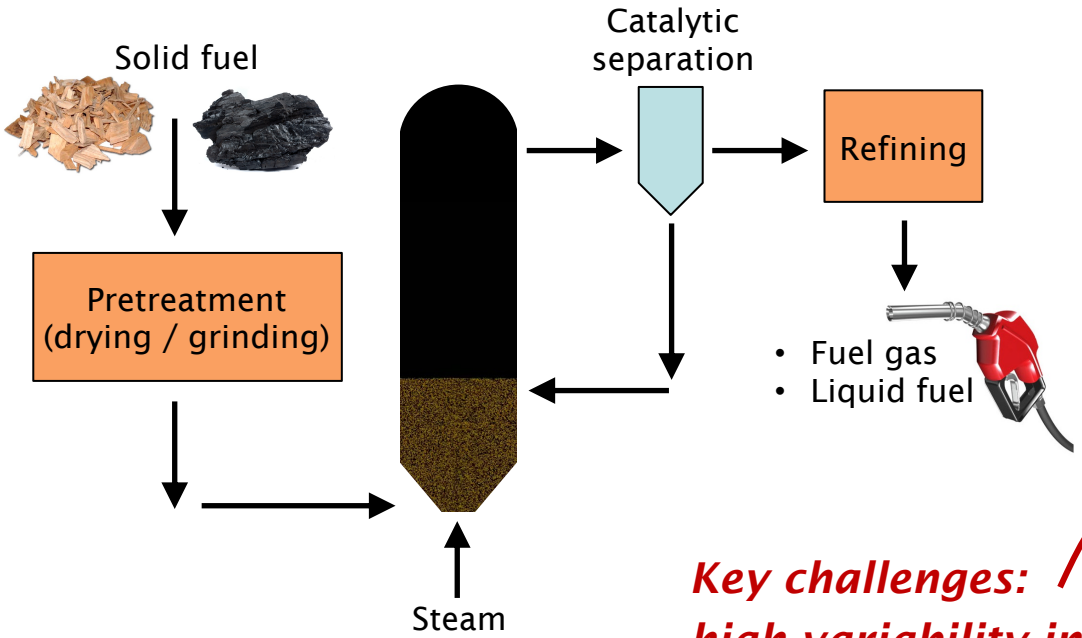

Reported hydrogen-to-carbon monoxide ratios

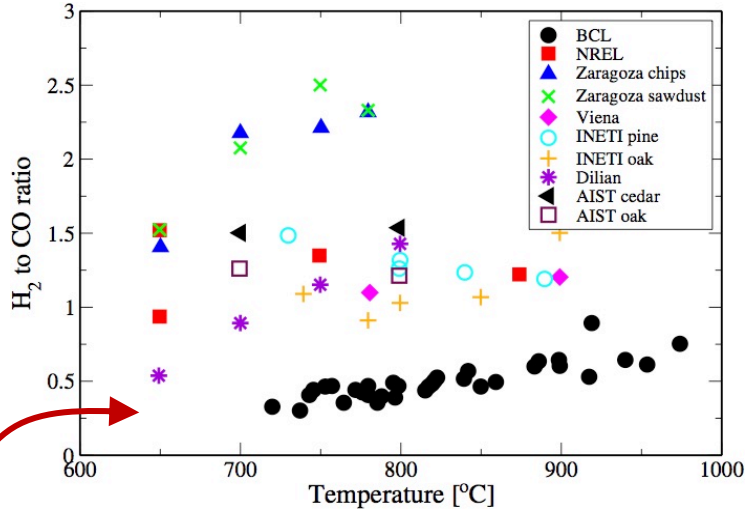

Key challenges:
high variability in reactor performance

Wall deposition contributes to reactor performance variations

Cohesion and deposition of Geldart-A/C particles significantly impact the reactor performance

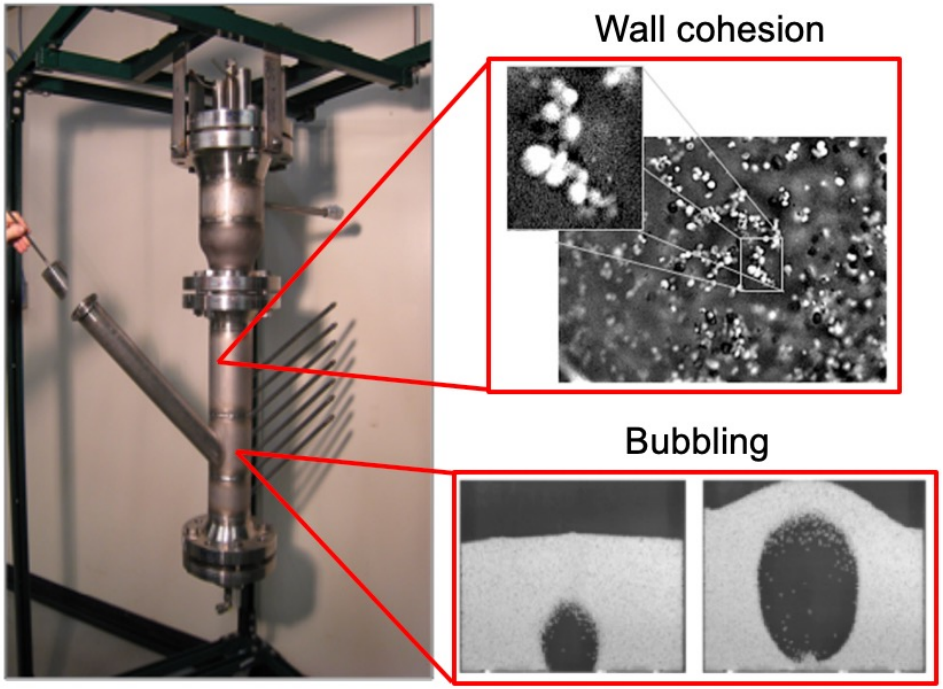

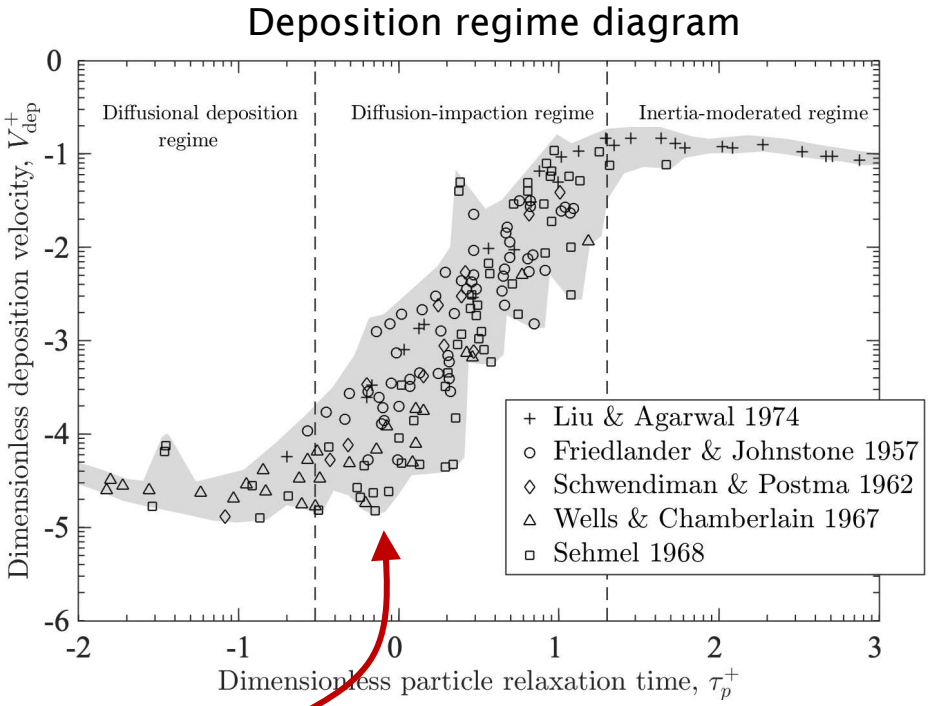

Large uncertainties observed from experimental measurements

Large underlying uncertainties in particle material properties

The physical properties of Geldart-A/C (e.g., catalyst, dust) particles can vary by orders of magnitude, which pose further modeling challenges

Particle types	d_p [μm]	Hamaker constant [1e-20 J]		Electric charge [C]	CoR
		A_{11}	A_{12}		
SiO_2 (Silica)	0.1 – 100	6.5	5.37 – 13.7	8.0e-18 – 4.0e-16	0.62 – 0.77
SiO_2 (Quartz)	0.5 – 15	8.86	7.59 – 12.1	8.0e-18 – 4.0e-16	0.19
Al_2O_3 (Alumina)	0.2 – 34	15.2	7.90 – 21.1	1.4e-18 – 2.4e-16	0.62
$CaSO_4$ (Gypsum)	0.7 – 20	–	–	–	0.10
Dolomite	2 – 40	7.34 – 13.75	–	–	0.15
NaCl (Salt)	–	6.48	6.45 – 10.3	–	0.11
Fe_2O_3	–	6.8 – 25	–	–	–
MgO	–	10.6 – 12.1	8.84 – 14.2	–	–
CaO	–	12.4	–	–	–
TiO_2	–	15.3	9.46 – 15.4	–	–
ARD	1 – 40	1.76 – 125	N/A	1.08e-17 – 5.2e-16	0.34 – 0.76
Fly ash	1.5 – 80	0.25 – 1.9	N/A	8.7e-17 – 2.2e-16	0.16 – 0.75
Fine soil	2 – 20	1.05 – 513	N/A	2.3e-17 – 2.5e-16	0.38 – 0.92

Large underlying uncertainties in particle material properties

The physical properties of Geldart-A/C (e.g., catalyst, dust) particles can vary by orders of magnitude, which pose further modeling challenges

Main objectives:

1. Develop particle deposition models of different fidelity to predict deposition rate in the presence of cohesion
2. Quantify the uncertainties and sensitivities of deposition on cohesion strength efficiently by leveraging these models
3. Understand the role of temperature on deposition rates

Fly ash	1.5 – 80	0.25 – 1.9	N/A	8.7e-17 – 2.2e-16	0.16 – 0.75
Fine soil	2 – 20	1.05 – 513	N/A	2.3e-17 – 2.5e-16	0.38 – 0.92

A unit test case for particle deposition UQ and sensitivity analysis

$$D = 20 \text{ mm} \quad L = 10D \quad U_b = 4.0 \text{ m/s}$$

$$\varepsilon_p = 6.25 \times 10^{-7} \quad \rho_p = 2650 \text{ kg/m}^3$$

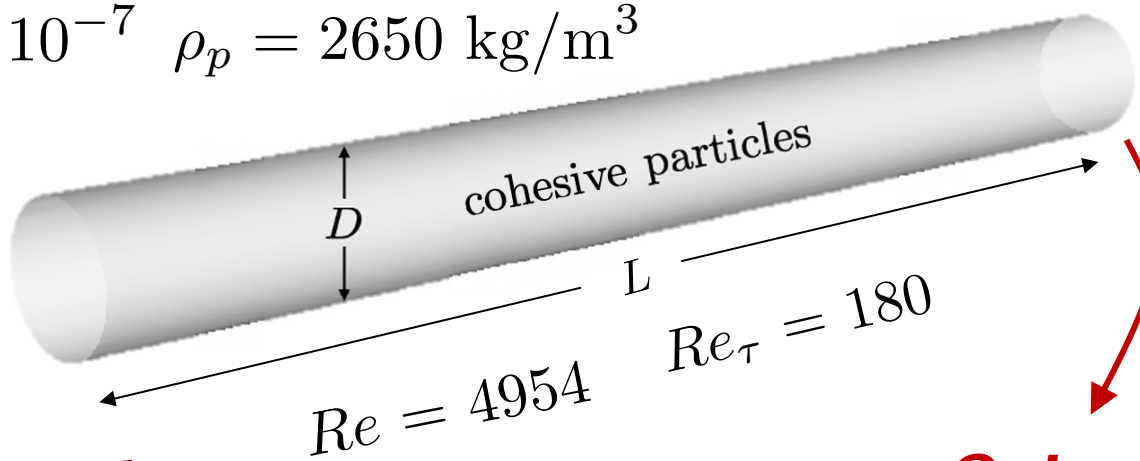

Input parameters:

$$\xi = q_p / q_{\max} \in [0, 0.1]$$

$$q_{\max} = 500 \times \left(1.6 \times 10^{-19}\right) \left(d_p / 10^{-6}\right)^2$$

$$\zeta = A / A_0 \in [0, 1]$$

$$A_0 = 1.0 \times 10^{-18}$$

QoI:

$$V_{\text{dep}}^{+} \equiv \frac{V_{\text{dep}}}{u_*} = \frac{J_w}{\rho_{pm} u_*}$$

Statistics:

- Mean
- Variance
- Sobol index

High-fidelity model – DNS-DEM framework

- NGA[1]
  - Finite volume DNS code
  - Massively parallel
  - Conservation of mass, momentum, and kinetic energy

Need to compute efficiently!
[Yao & Capecelatro (2018) PRF][3]
[Yao & Capecelatro (2021) JFM][4]

- Lagrangian particle tracking[2]
  - Position: $$\frac{d\boldsymbol{x}_p^{(i)}}{dt} = \boldsymbol{v}_p^{(i)}$$
  - Velocity: $$m_p \frac{d\boldsymbol{v}_p^{(i)}}{dt} = \underline{\boldsymbol{F}_{\text{drag}}^{(i)}} + \underline{\boldsymbol{F}_{\text{col}}^{(i)}} + \underline{\boldsymbol{F}_{\text{vw}}^{(i)} + \boldsymbol{F}_{\text{coulomb}}^{(i)}}$$
  - Angular velocity: $$I_p \frac{d\boldsymbol{\omega}_p^{(i)}}{dt} = \sum_j \frac{d_p}{2} \boldsymbol{n}_{ij} \times \underline{\boldsymbol{f}_{t,j\to i}^{\text{col}}}$$

Collisions: Soft-sphere (mass-spring-damper)

Drag: Tenneti et al. (2011)

Collisions: Coulomb friction

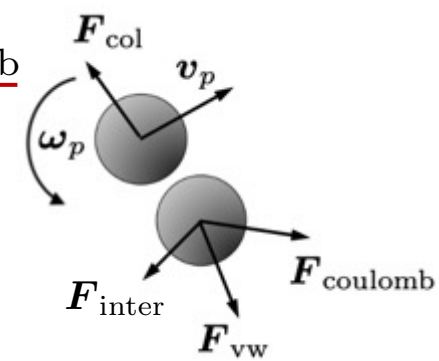

1. O. Desjardins et al. (2008), JCP.
2. J. Capecelatro and O. Desjardins. (2013), JCP, 238:1–31.
3. Y. Yao and J. Capecelatro. (2018), PRF, 3(3):034301.
4. Y. Yao and J. Capecelatro. (2021), JFM, 911, A10.

A brief note on the electrostatics and van der Waals algorithms

An accurate electrostatic algorithm – P3M:

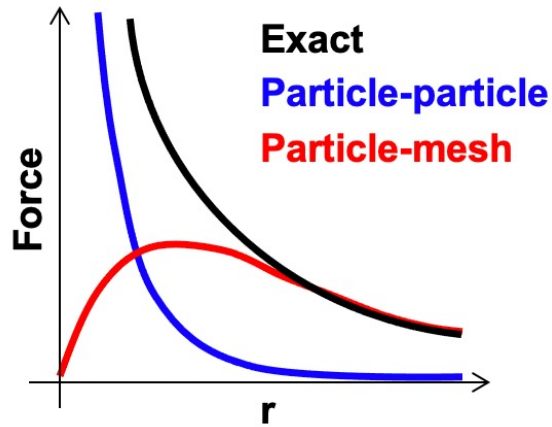

Efficient using FFT

Long range:

$$\boldsymbol{E}_l(\boldsymbol{x},t) = -\nabla\phi(\boldsymbol{x},t) \quad k^2\hat{\phi}_l(\boldsymbol{k}) = \frac{\hat{\rho}_l(\boldsymbol{k})}{\epsilon_0}$$

Short range: if $r_{ij} < r_{\max}$

$$F_s(r_{ij}) = q_i q_j/(4\pi\epsilon_0 r_{ij}^2) - F_d(r_{ij})$$

Double counting removed

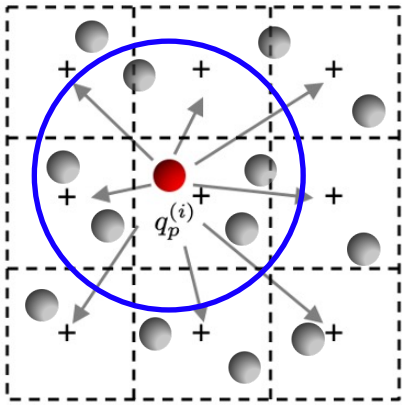

Van der Waals (Hamaker 1937)[1]: $F_{vdw}(A,s) = \frac{A}{3}\frac{2r_ir_j(r_i+r_j+s)}{s^2(2r_i+2r_j+s)^2}\left[\frac{s(2r_i+2r_j+s)}{(r_i+r_j+s)^2-(r_i-r_j)^2}-1\right]^2$

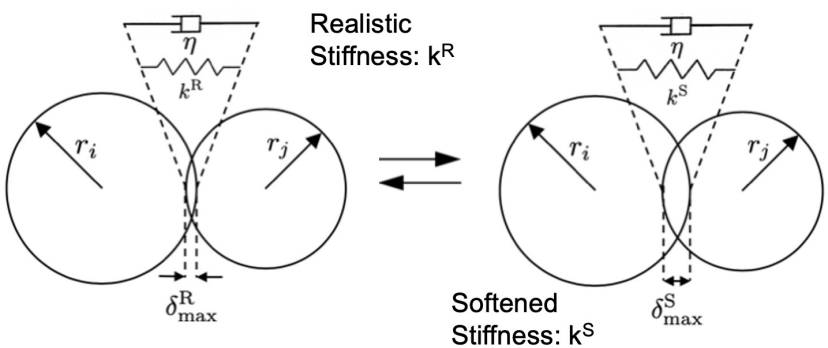

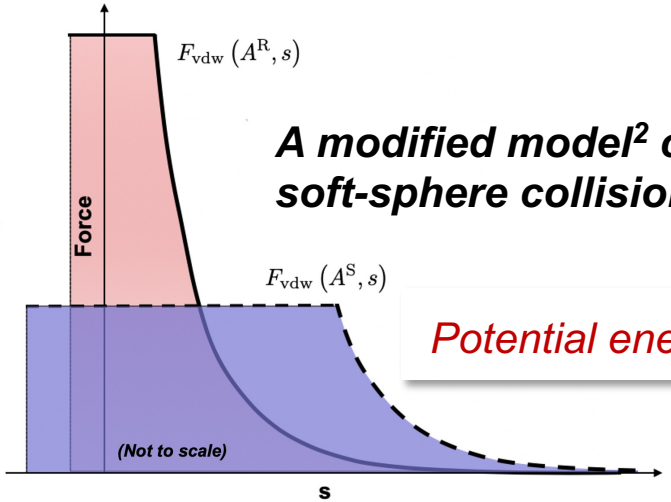

A modified model[2] compatible with soft-sphere collisions is employed

Potential energy is conserved

1. H. C. Hamaker. (1937), *Physica*.
2. Y. Gu et al. (2016), *Powder Tech*.

High-fidelity model – DNS-DEM framework

DNS of a turbulent pipe flow

$10D \times D \times D$

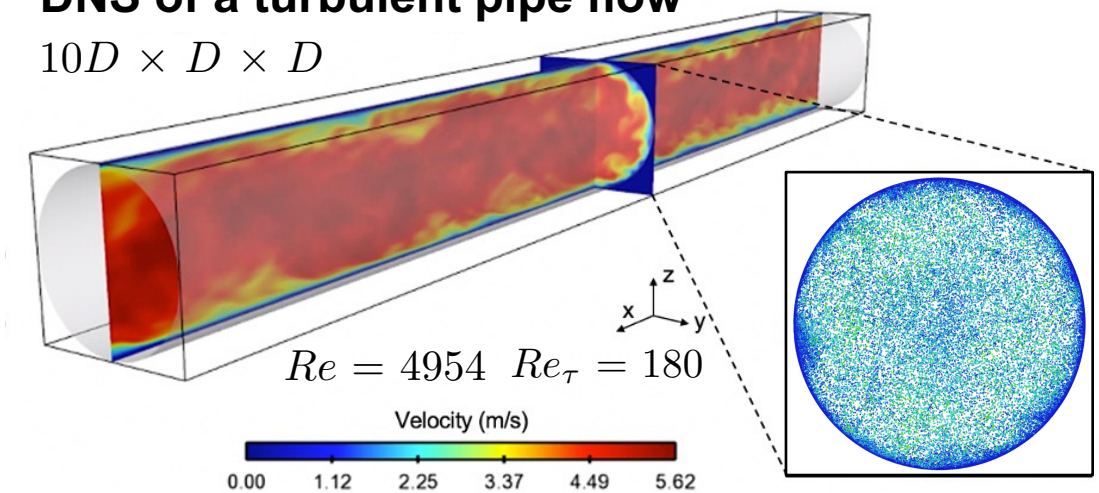

$\text{grid} = 326 \times 256 \times 256$

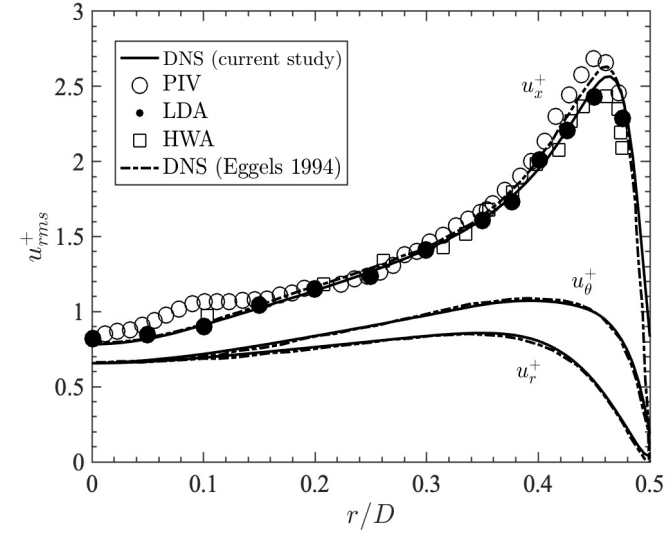

- Non-dimensional deposition rate:

$$V_{\text{dep}}^+ = \left(\frac{\Delta N_{\text{dep}} D}{4 \Delta t \left(N_0 - \Delta N_{\text{dep}} \right)} \right) / u_*$$

- Particles counted as deposited once they hit the wall (all-stick assumption)
- 256 CPU hours required for converged statistics for each set of inputs (ζ, ξ)

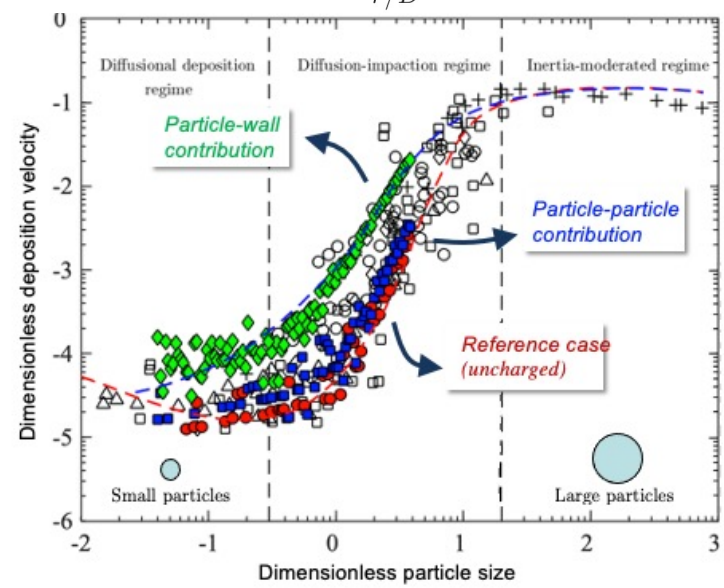

Low-fidelity model – 1D Eulerian conservation equations

- A 1D Eulerian-based model by Guha[1] predicts deposition reasonably well, which is leveraged here to provide 'low-fidelity' predictions.

Momentum: $$\bar{V}_{py}^{+}\frac{\partial \bar{V}_{py}^{+}}{\partial y^{+}} + \frac{\bar{V}_{py}^{+}}{\tau_p^{+}} = -\frac{\partial}{\partial y^{+}}\left(\Re\overline{V_{fy}'^{+2}}\right) + F_{\mathrm{elec}}^{+} + F_{\mathrm{vdw}}^{+}$$

Mass: $$\partial V_{\mathrm{dep}}^{+}/\partial y^{+} = 0, \quad V_{\mathrm{dep}}^{+} = -\left(\frac{D_{\mathrm{B}}}{\nu} + \frac{\varepsilon}{\nu}\right)\frac{\partial \rho_p^{+}}{\partial y^{+}} + \rho_p^{+}\bar{V}_{py}^{+}$$

Electrical charge

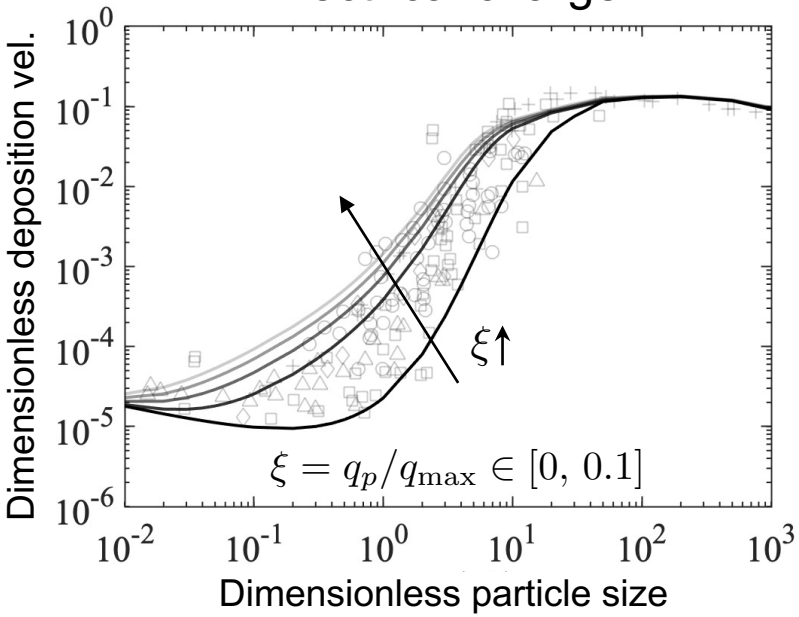

Van der Waals force

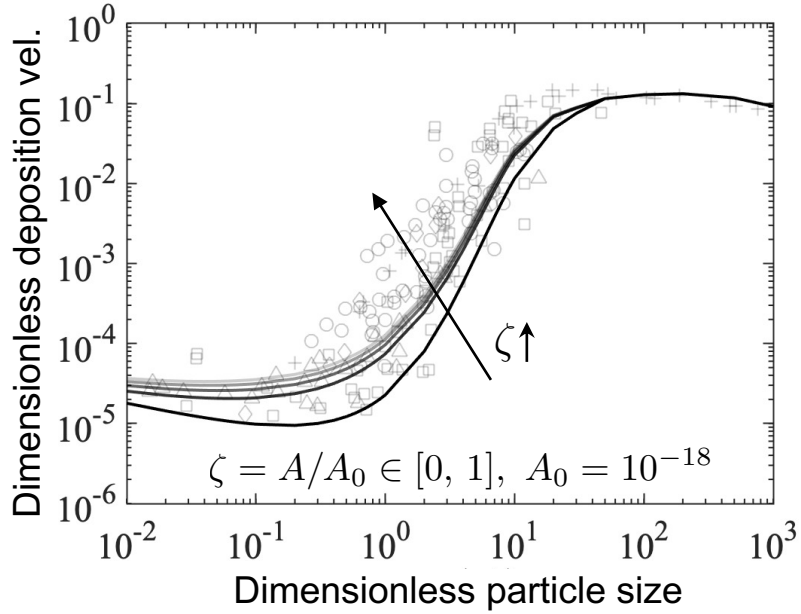

1. A. Guha. (2008), *Annu. Rev. Fluid Mech.*

Multi-fidelity uncertainty quantification[1]

- ***Goal: quantify how deposition rate depends on uncertainties in charge and van der Waals efficiently***

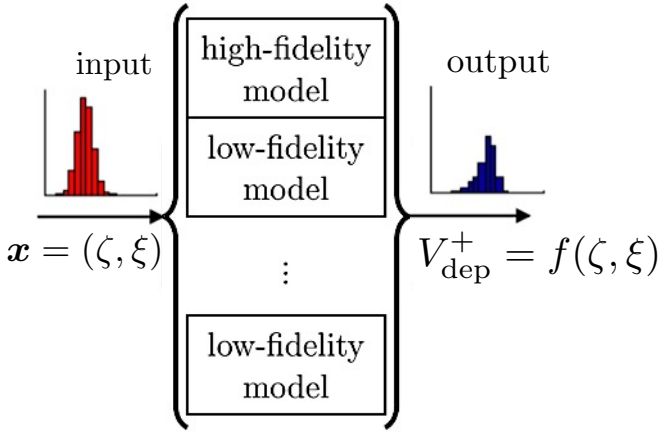

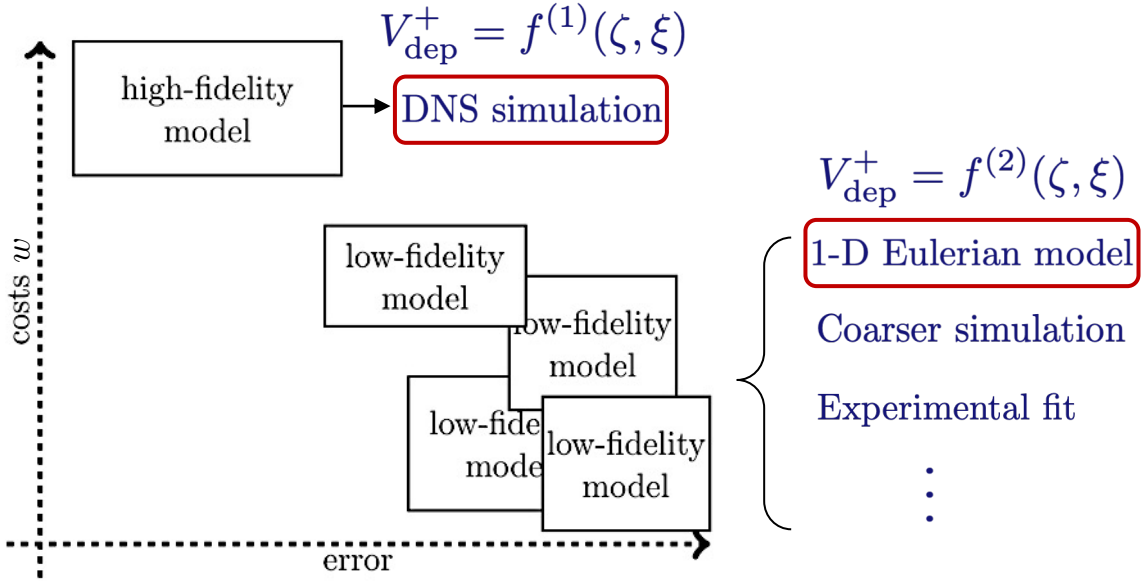

- Classic Monte Carlo (MC) estimator: $\bar{y}_{m_1} = \frac{1}{m_1} \sum_{j=1}^{m_1} f^{(1)}(\boldsymbol{x}_j)\,,\ \bar{y}_{m_2} = \frac{1}{m_2} \sum_{j=1}^{m_2} f^{(2)}(\boldsymbol{x}_j)$
- Multi-fidelity Monte Carlo (MFMC) estimator: $\hat{s} = \bar{y}_{m_1} + \alpha_2 \left(\bar{y}_{m_2}^{(2)} - \bar{y}_{m_1}^{(2)} \right)$

Find the optimal m_1, m_2, $\boldsymbol{\alpha}_2$ to minimize estimator error under the constraint: $m_1 w_1 + m_2 w_2 \leq p$

1. Peherstorfer et al. (2018), *Siam Review*.

1D Eulerian model underpredicts deposition compared to DNS

Prior estimates of model statistics:

- DNS: ~256 CPU hours

$$w_1 = 1$$

- 1D model: ~0.08 CPU hour

$$w_2 = 1/2880$$

- Correlation coefficients:

$$\rho_{1,2} = \frac{\mathrm{Cov}\left[f^{(1)}(X), f^{(2)}(X)\right]}{\sigma_1 \sigma_2}$$

An analytical solution exists for the MFMC optimization[1]!

$$(\alpha_2, m_1, m_2) = \mathrm{MFMC}\left(\rho_{1,2}, w_1, w_2, \sigma_1, \sigma_2\right)$$

$$\hat{s}_{\mathrm{MFMC}} = \hat{s}_{\mathrm{MC},m_1} + \alpha_2 \left(\hat{s}^{(2)}_{\mathrm{MC},m_2} - \hat{s}^{(2)}_{\mathrm{MC},m_1}\right)$$

- Comparison of deposition predictions from DNS and 1D model

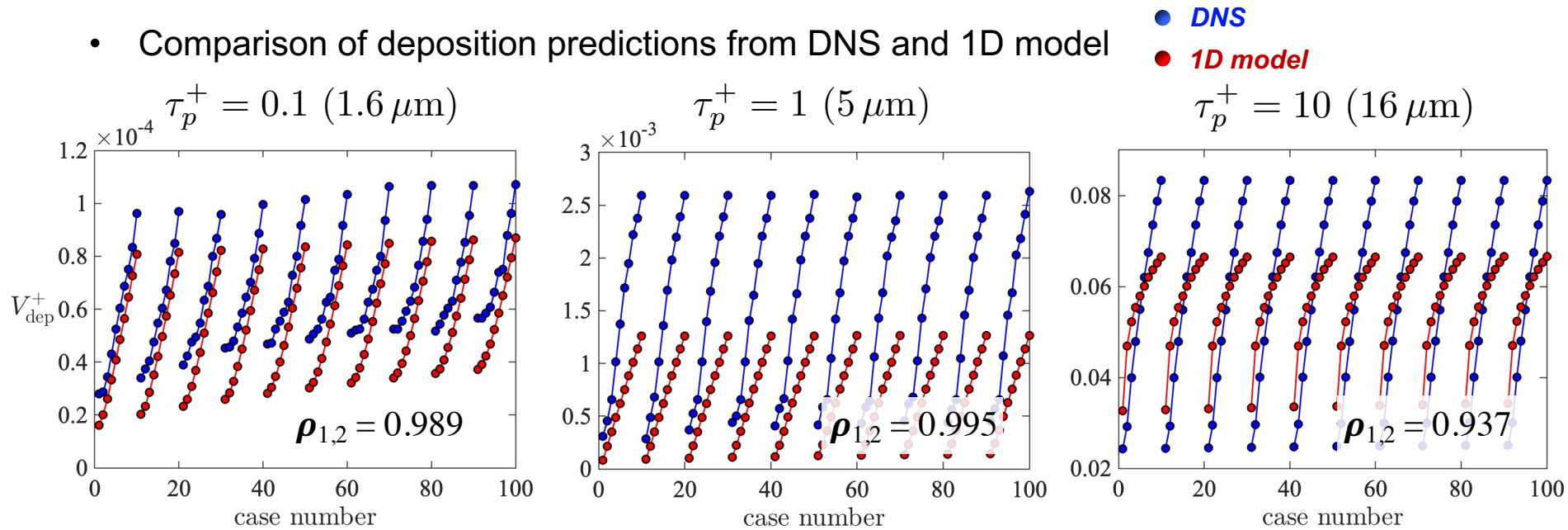

1. Peherstorfer et al. (2018), *Siam Review*.

Solution procedure of MFMC UQ on deposition rates

DNS simulations

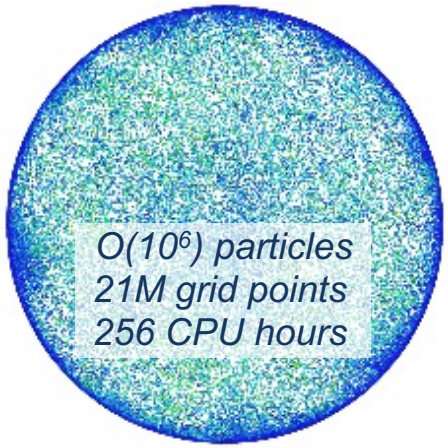

Input sampling

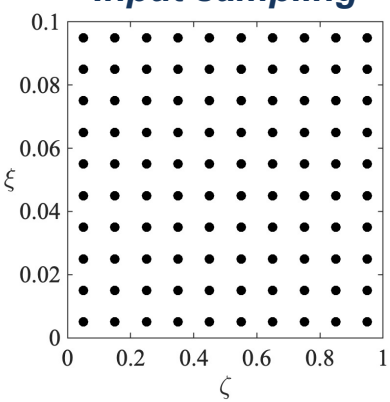

$\xi \in [0, 0.1] \quad \zeta \in [0,\ 1]$

MFMC optimization

$$V_{\text{dep}}^{+} = f^{1,2}(\zeta, \xi)$$

MFMC estimator

Low-fidelity simulations

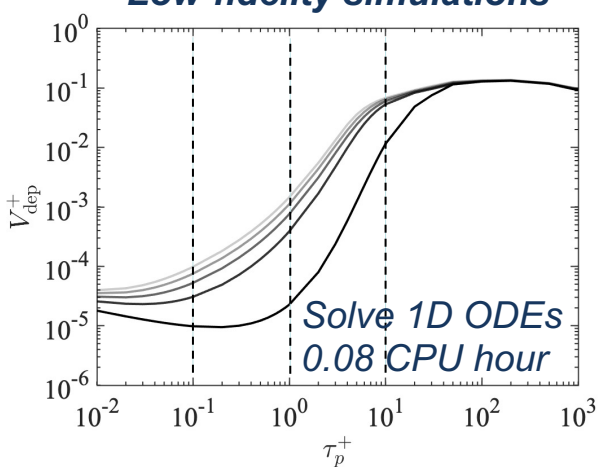

Statistical estimates (mean, SD, sensitivity)

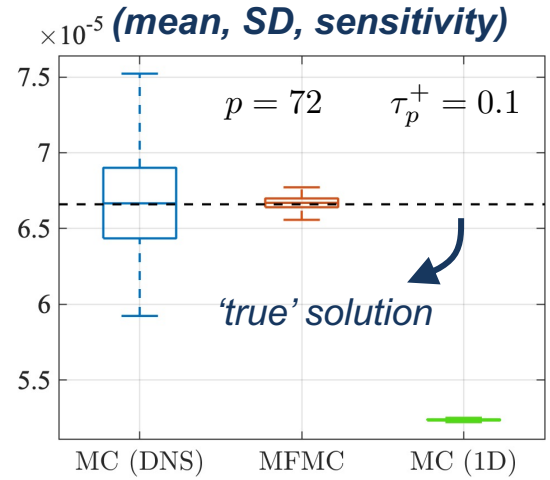

Benefits of MFMC:

- Smaller variance than pure DNS
- Less bias compared to 1D model

Uncertainty and sensitivity of deposition for three particle sizes

Mean, standard deviation, and sensitivity of deposition rate are estimated using the multi-fidelity approach with budget p=144 (~40,000 CPU hours)

Uncertainty (mean + SD)

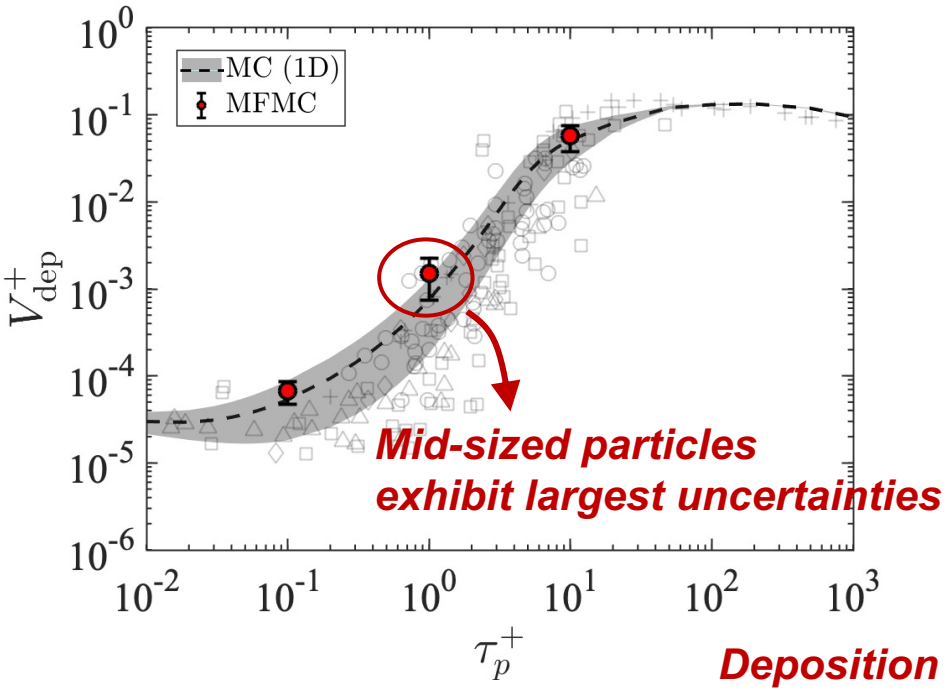

Sensitivity of deposition rate

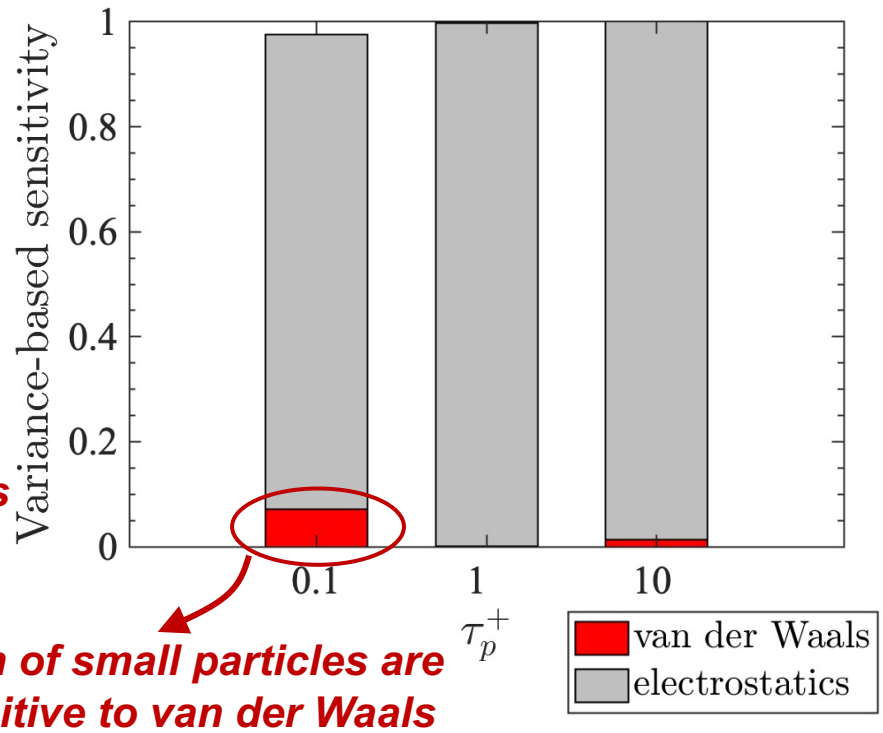

Effect of cohesion and temperature on particle rebound

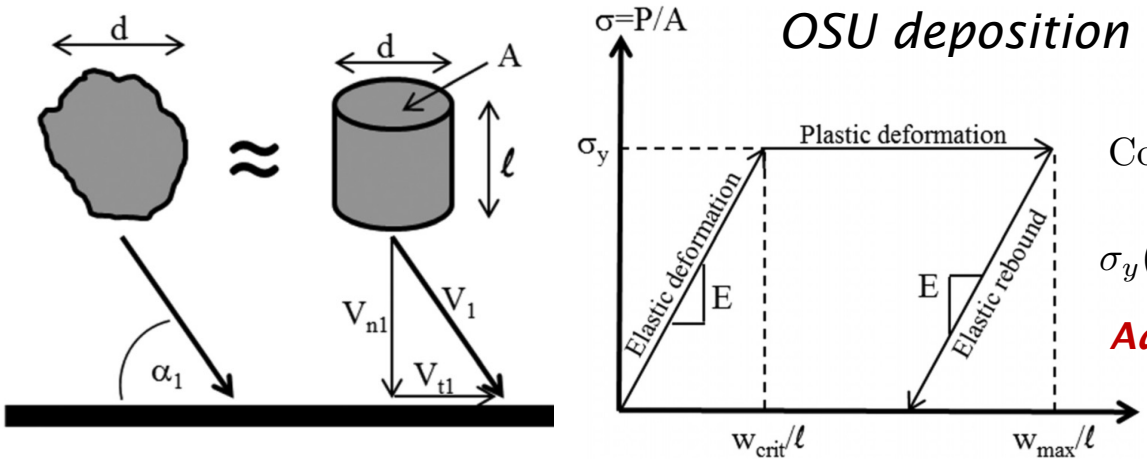

OSU deposition model (Bons et al 2017):

$$\mathrm{CoR}_n = \frac{V_{n2}}{V_{n1}} = \sqrt{\frac{\sigma_y^2}{\rho E} - \frac{2A_{\mathrm{cont}}\gamma}{m}}\frac{1}{V_{n1}}$$

$$\sigma_y(T) = 200 - 0.225(T - 1000)\ (\mathrm{MPa})$$

Additional input parameter:

$$\theta = 0.225(T - 1000)/200 \in [0, 1]$$

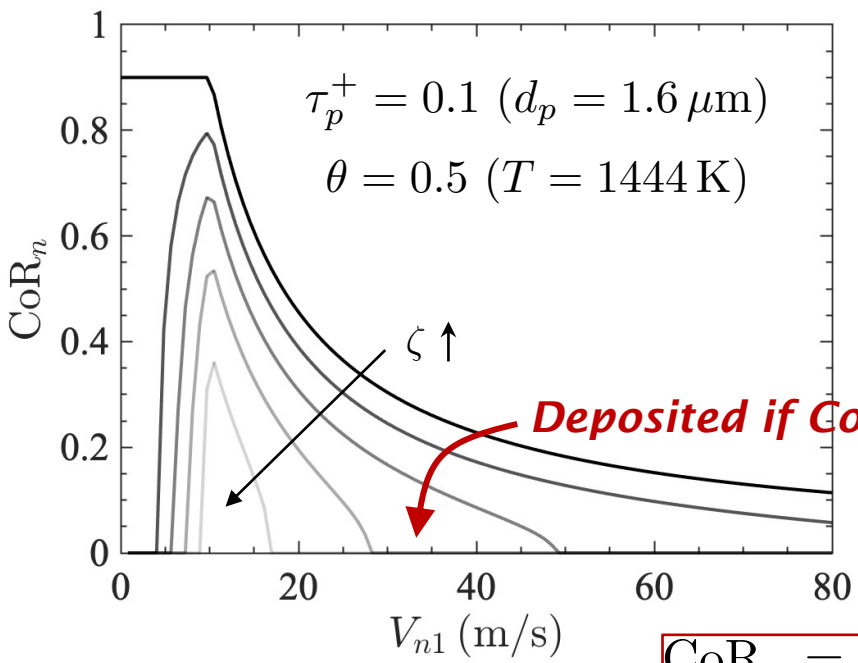

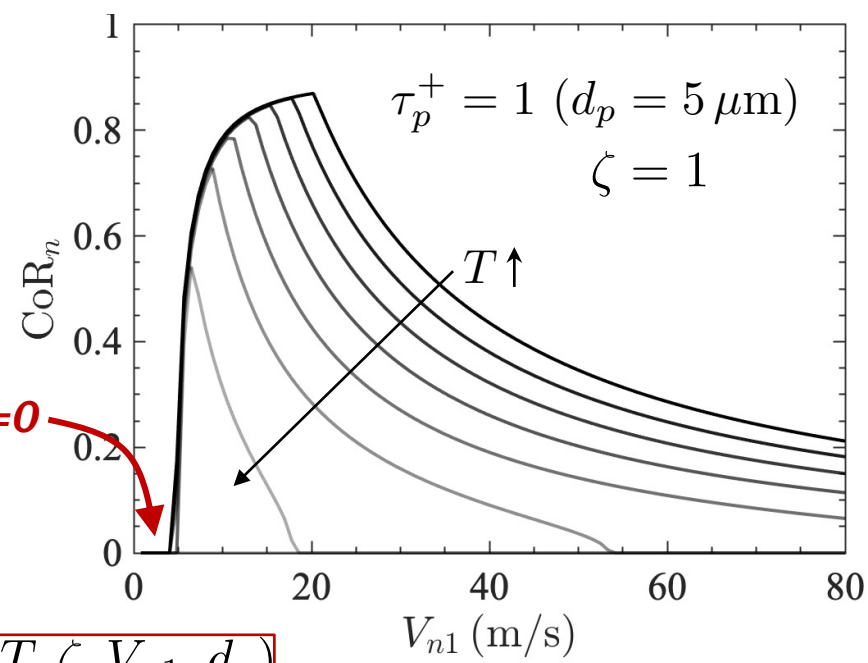

Deposited if CoR=0

$$\mathrm{CoR}_n = f(T, \zeta, V_{n1}, d_p)$$

Sensitivity of Capture Efficiency (CE) on temperature

- 1D model and DNS are modified to include OSU deposition model
- Capture efficiency is typically measured in experiments:

$$CE = \frac{\dot{m}_{\mathrm{dep}}}{\dot{m}_{\mathrm{tot}}} = \frac{4L}{D}\frac{u_*}{U_b}V^+_{\mathrm{dep}}$$

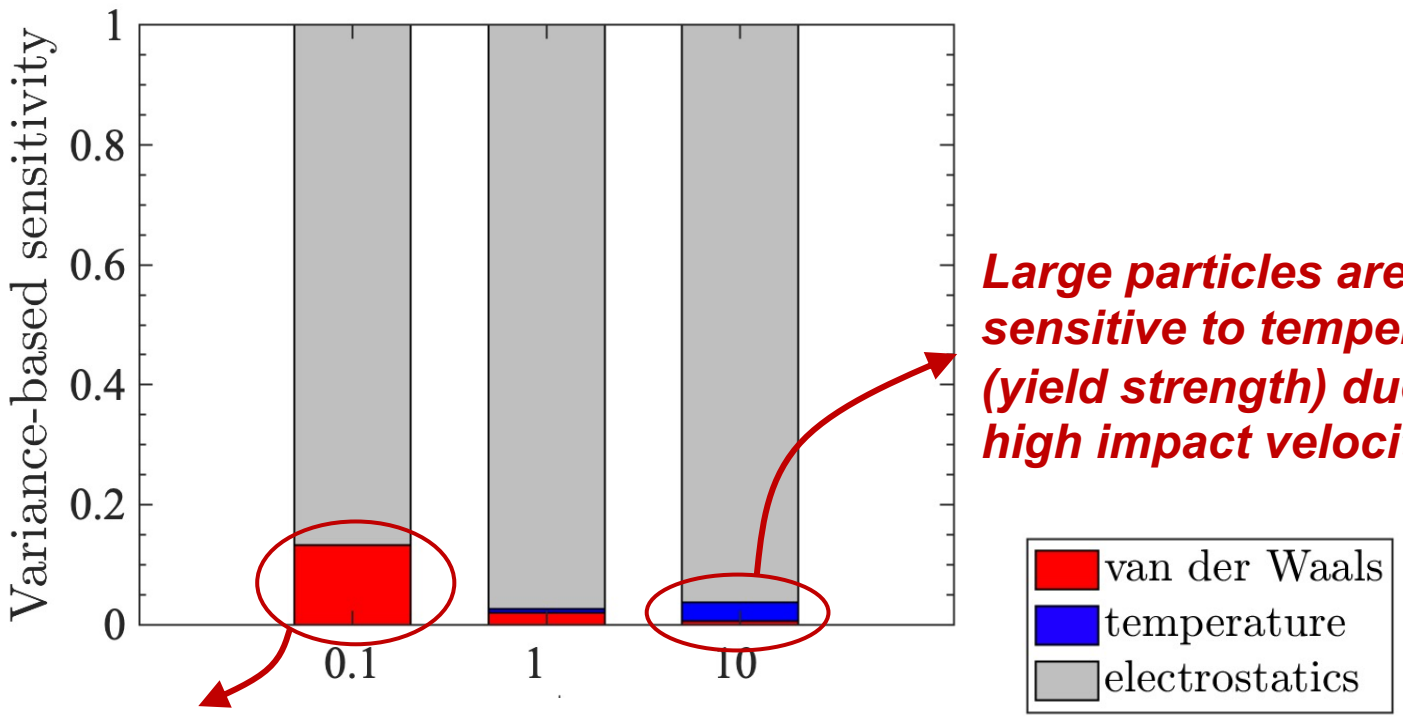

Large particles are more sensitive to temperature (yield strength) due to high impact velocity

Small particles are even more sensitive to van der Waals as adhesion is accounted for in rebound

Conclusions

1. A **multi-fidelity** approach was employed to optimally estimate **mean**, **variance**, and **sensitivity** of the deposition rate.

    - Cheap 1D models were evaluated to reduce the cost while retaining accuracy guarantees of expensive DNS.

2. Deposition was found more sensitive to **electrostatics** than van der Waals across all particle sizes and exhibited largest uncertainty for **mid-sized** particles.

3. **All-stick** assumption is more valid for **small particles** whose deposition is more sensitive to cohesion and less sensitive to temperature

Questions?

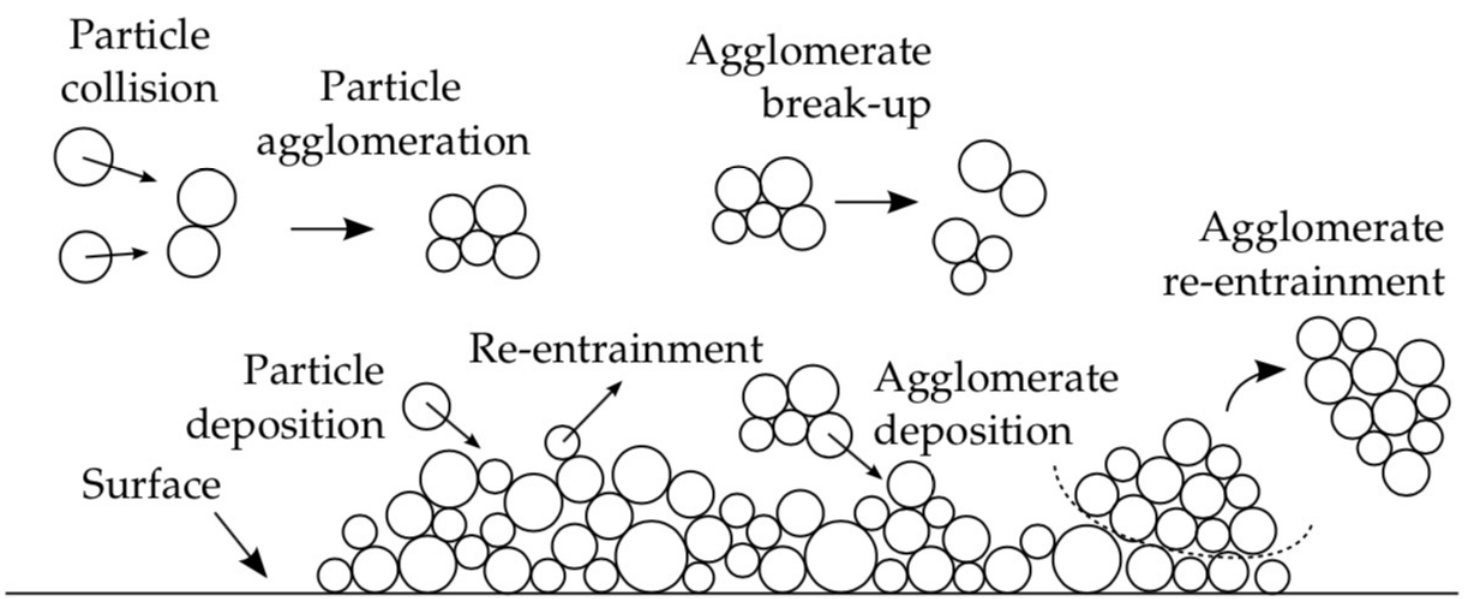

Credit: Jakob Haervig

Uncertainties of deposition rate to charge and van der Waals

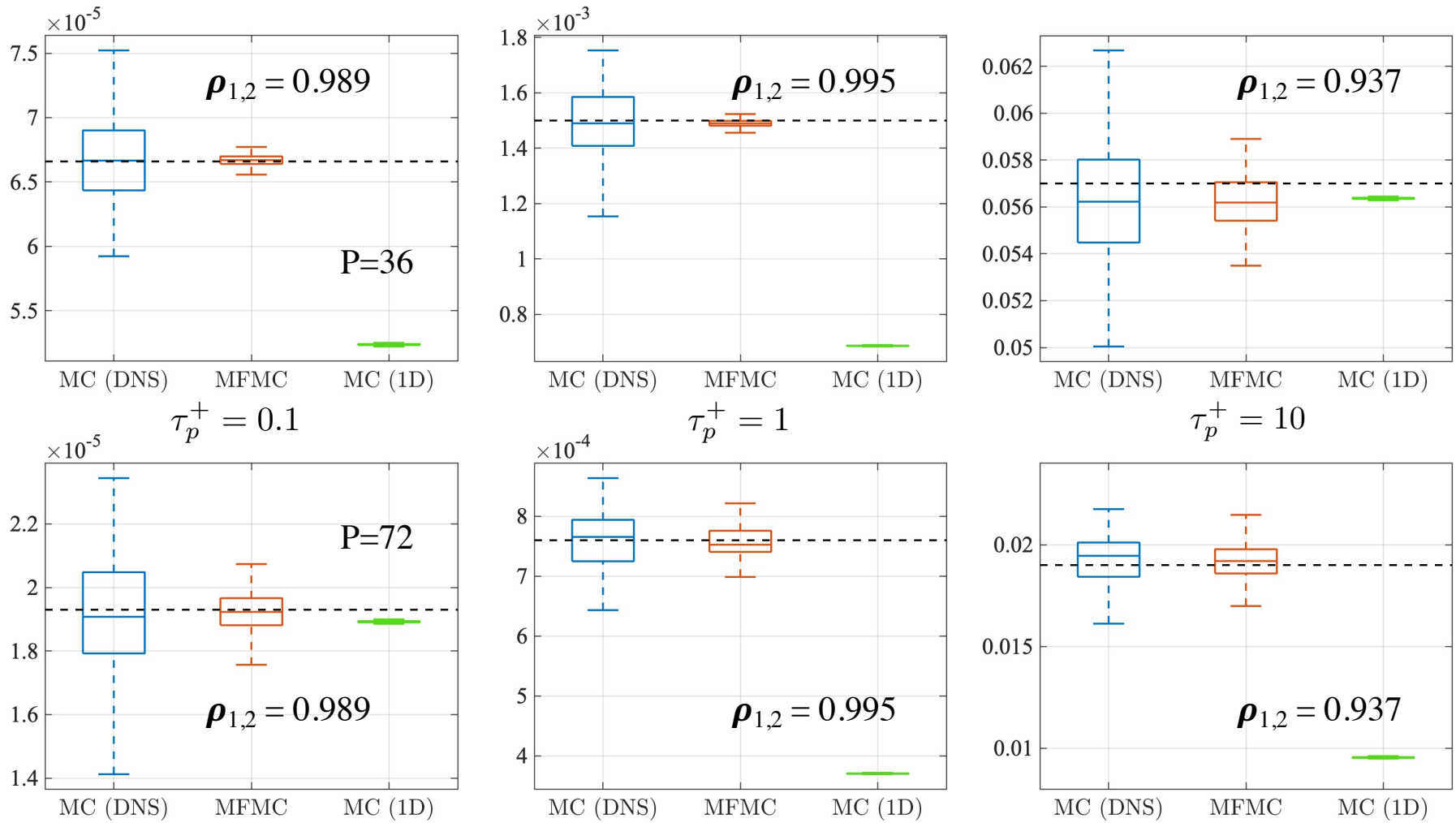

Sensitivity of deposition rate to charge and van der Waals

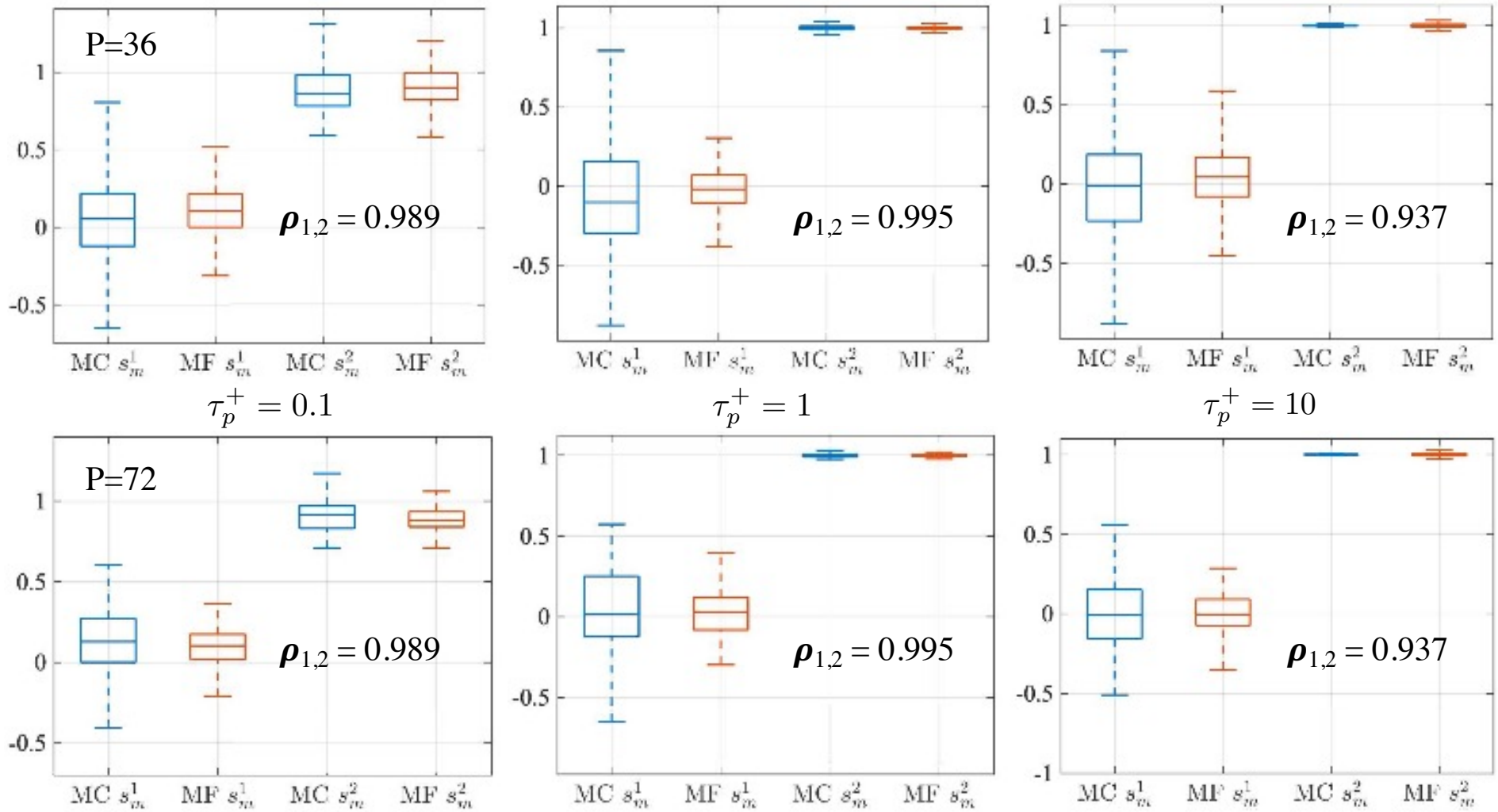

Multi-fidelity Uncertainty Quantification

- An analytical solution exists for the optimal number of evaluations for each model

Algorithm 2. Multifidelity Monte Carlo.

procedure MFMC($f^{(1)}, \ldots, f^{(k)}, \bar{\sigma}_1, \ldots, \bar{\sigma}_k, \bar{\rho}_{1,1}, \ldots, \bar{\rho}_{1,k}, w_1, \ldots, w_k, p$)

Ensure $f^{(1)}, \ldots, f^{(k)}$ is the result of MSELECT defined in Algorithm 1

Set $\bar{\rho}_{1,k+1} = 0$ and define vector $\bar{\boldsymbol{r}} = [\bar{r}_1, \ldots, \bar{r}_k]^T \in \mathbb{R}_+^k$ as

$$\bar{r}_i = \sqrt{\frac{w_1(\bar{\rho}_{1,i}^2 - \bar{\rho}_{1,i+1}^2)}{w_i(1 - \bar{\rho}_{1,2}^2)}}, \qquad i = 1, \ldots, k$$

Select number of model evaluations $\boldsymbol{m} \in \mathbb{R}_+^k$ as

$$\boldsymbol{m} = \left[\frac{p}{\boldsymbol{w}^T \bar{\boldsymbol{r}}}, \bar{r}_2 m_1, \ldots, \bar{r}_k m_1\right]^T \in \mathbb{R}_+^k$$

Round down components of $\boldsymbol{m}$ to obtain integers

Set coefficients $\boldsymbol{\alpha} = [\alpha_1, \ldots, \alpha_k]^T \in \mathbb{R}^k$ to

$$\alpha_i = \frac{\bar{\rho}_{1,i}\bar{\sigma}_1}{\bar{\sigma}_i}, \qquad i = 1, \ldots, k$$

Draw $\boldsymbol{z}_1, \ldots, \boldsymbol{z}_{m_k} \in \mathcal{D}$ realizations of Z

Evaluate model $f^{(i)}$ at realizations $\boldsymbol{z}_1, \ldots, \boldsymbol{z}_{m_i}$ for $i = 1, \ldots, k$

Compute MFMC estimate $\hat{s}$ as in (3.2)

return $\hat{s}$

end procedure

- Advantages:
  - Orders of magnitudes faster than normal UQ
  - Low-fidelity models can take any forms: ROM, coarser mesh, POD/DMD, line fitting etc….
  - Error for each level of model is not required for MFMC UQ

Reduced variance by leveraging models of different fidelities

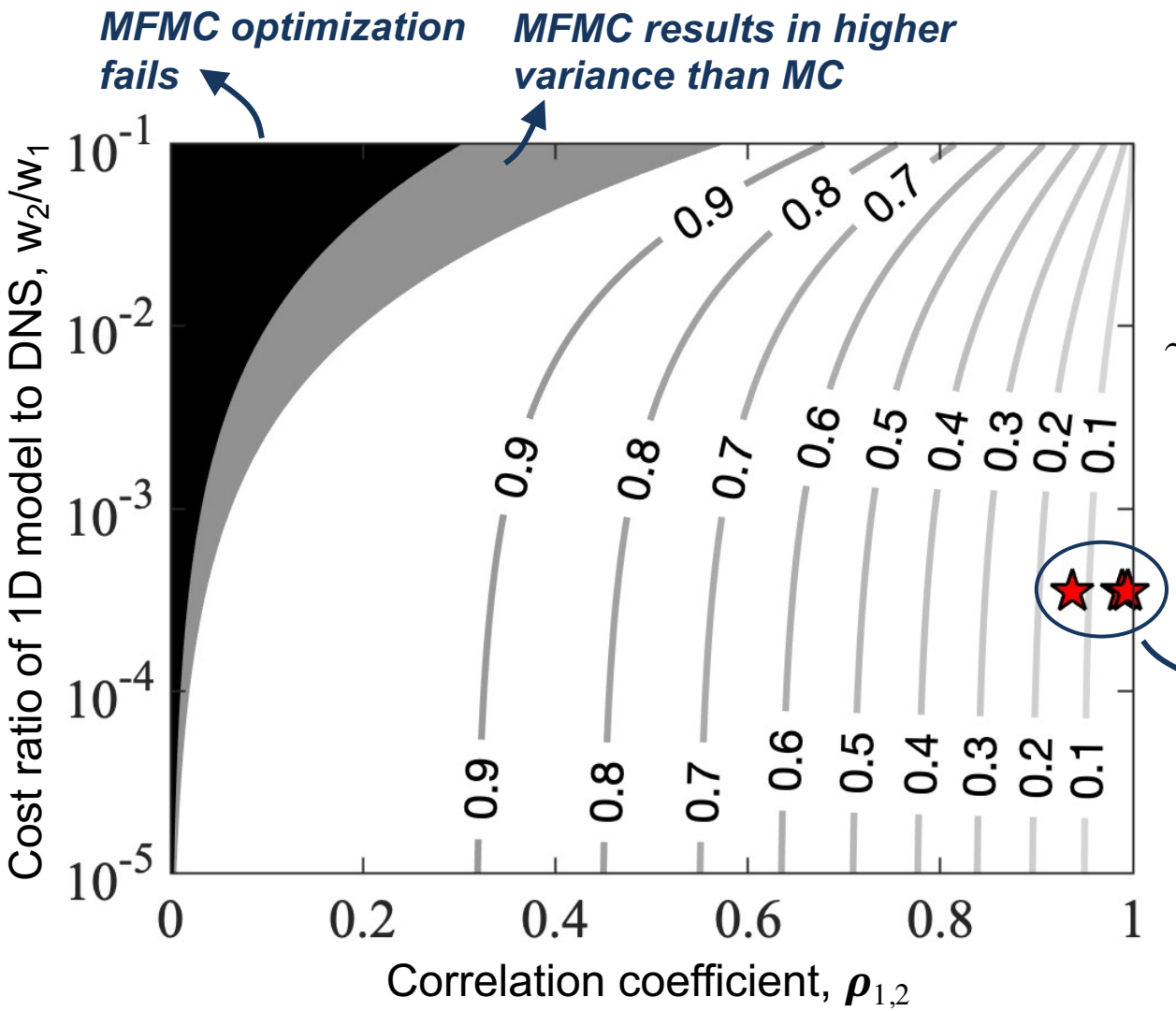

Variance reduction ratio[1]:

$$\gamma = \left(\sqrt{1-\rho_{12}^2} + \rho_{12}\sqrt{w_2/w_1}\right)^2$$

$$\tau_p^+ = 0.1, 1, 10$$

An order of magnitude reduction in the variance!

1. Peherstorfer et al. (2018), *Siam Review*.

Charge modifies particle near-wall statistics[1]

DNS of a turbulent pipe flow

$10D \times D \times D$

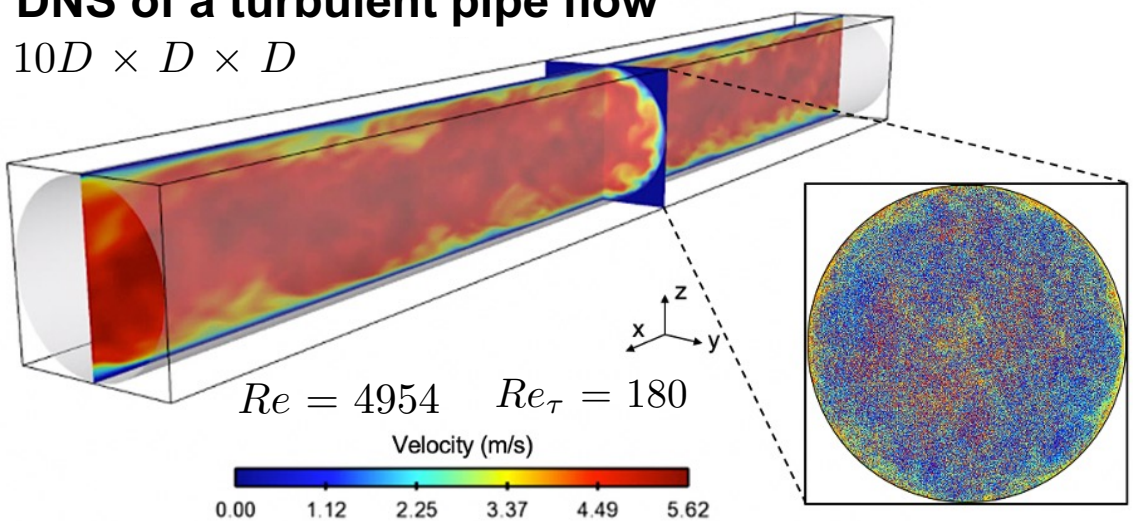

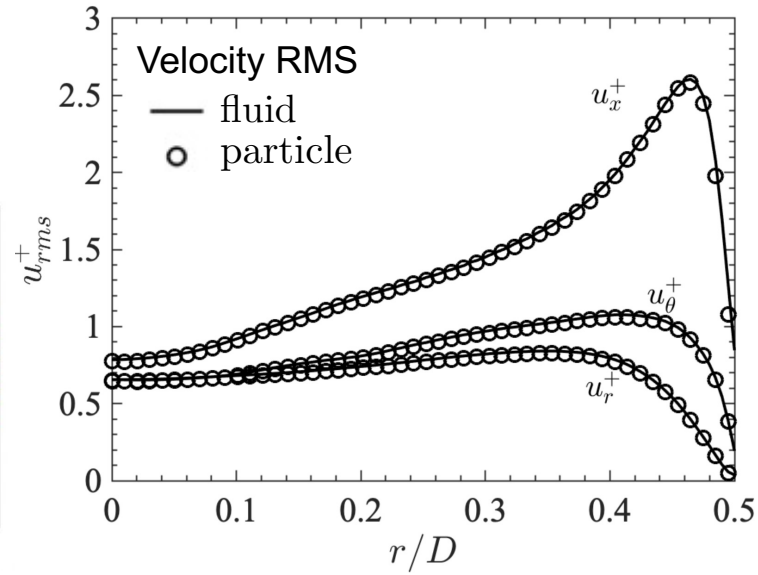

Number density (uncharged)

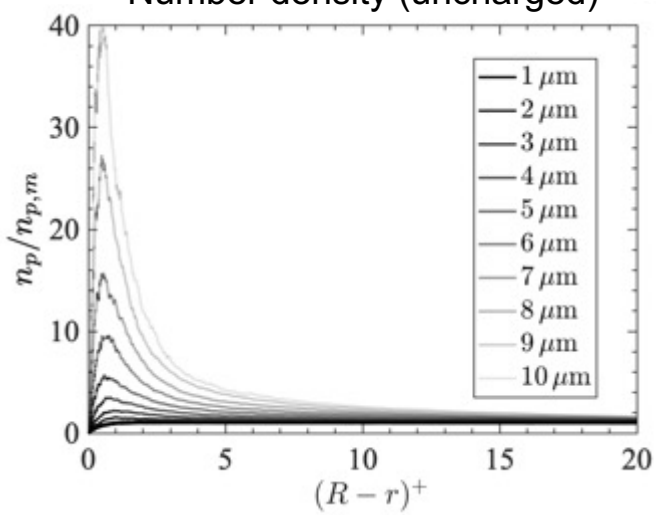

Number density (charged)

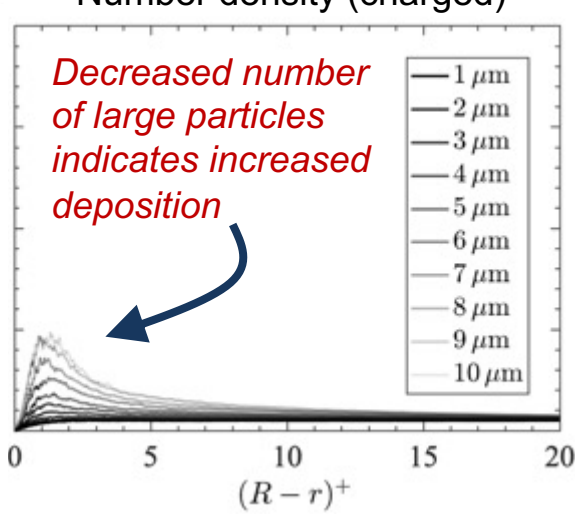

$\xi = 0.1$, w/ image charging

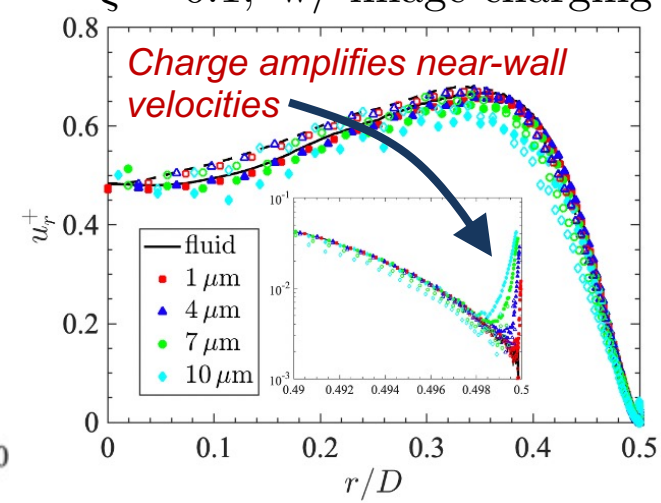

1. **Yao** & Capecelatro. (2021), *Powder Tech.*

Scaled-mapping treatment for non-periodic geometries

- Particles are scaled-mapped inwards by $\gamma = \mathcal{L}/D$ to remove periodic images[1]:

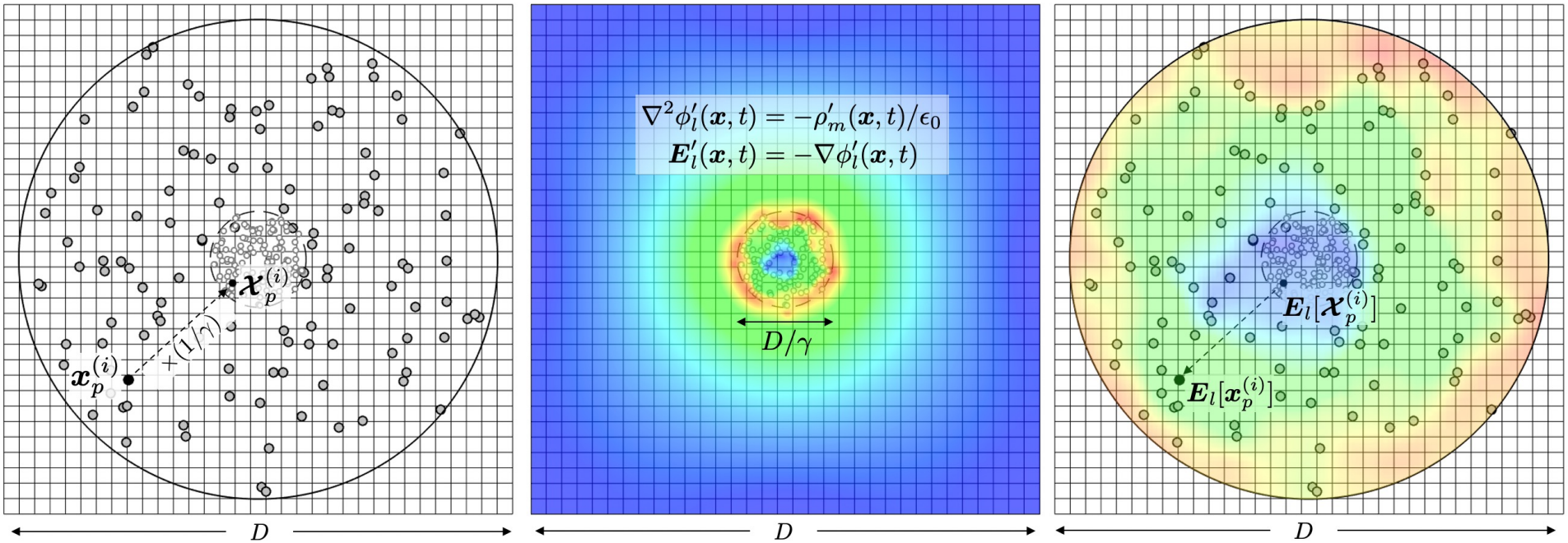

Step 1: particle scaled-mapping

$* \ \boldsymbol{\mathcal{X}}_p^{(i)} = \boldsymbol{x}_p^{(i)} \otimes (1, 1/\gamma, 1/\gamma)$

$$\rho_m'(\boldsymbol{x},t) = \sum_{i=1}^{N} q_p^{(i)} \mathcal{W}\left(\boldsymbol{x} - \boldsymbol{\mathcal{X}}_p^{(i)}(t)\right)$$

$* \ \rho_m(\boldsymbol{x},t) = \rho_m'(\boldsymbol{x},t)/\gamma^2$

Step 2: solve scaled electrical field

$$\hat{\rho}_l(\boldsymbol{k}) = \hat{\rho}_m(\boldsymbol{k})\hat{G}(\boldsymbol{k})$$

$$k^2\hat{\phi}_l(\boldsymbol{k}) = \frac{\hat{\rho}_l(\boldsymbol{k})}{\epsilon_0}$$

$$\boldsymbol{E}_l'(\boldsymbol{x},t) = -\nabla\phi_l(\boldsymbol{x},t)$$

Step 3: mapping the solutions back

$* \ \boldsymbol{E}_l(\boldsymbol{x},t) = \boldsymbol{E}_l'(\boldsymbol{x},t) \otimes (1, 1/\gamma, 1/\gamma)$

$* \ \boldsymbol{E}_l[\boldsymbol{x}_p^{(i)}] = \boldsymbol{E}_l[\boldsymbol{\mathcal{X}}_p^{(i)}]$

$*$ indicates additional steps

1. **Yao** & Capecelatro. (2021), *Powder Tech.*